Bi-Exponential Magnetic Resonance Signal Model for Partial Volume Computation

Quentin Duché[1,2,3,5], Oscar Acosta[1,2], Giulio Gambarota[1,2,3], Isabelle Merlet[1,2], Olivier Salvado[5], and Hervé Saint-Jalmes[1,2,3,4]

[1] Université de Rennes 1, LTSI - Rennes, F-35000, France
[2] INSERM, U1099 - Rennes, F-35000, France
[3] PRISM - Biosit, CNRS UMS 3480 - Biogenouest - Rennes, F-35000, France
[4] CRLCC, Centre Eugène Marquis - Rennes, F-35000, France
[5] CSIRO ICT Centre, The Australian E-Health Research Centre, Brisbane, Australia
quentin.duche@univ-rennes1.fr

Abstract. Accurate quantification of small structures in magnetic resonance (MR) images is often limited by partial volume (PV) effects which arise when more than one tissue type is present in a voxel. PV may be critical when dealing with changes in brain anatomy as the considered structures such as gray matter (GM) are of the similar size as the MR spatial resolution. To overcome the limitations imposed by PV effects and achieve subvoxel accuracy different methods have been proposed. Here, we describe a method to compute PV by modeling the MR signal with a biexponential linear combination representing the contribution of at most two tissues in each voxel. In a first step, we estimated the parameters (T1, T2 and Proton Density) per tissue. Then, based on the bi-exponential formulation one can retrieve fractional contents by solving a linear system of two equations with two unknowns, namely tissue magnetizations. Preliminary tests were conducted on images acquired on a specially designed physical phantom for the study of PV effects. Further, the model was tested on BrainWeb simulated brain images to estimate GM and white matter (WM) PV effects. Root Mean Squared Error was computed between the BrainWeb ground truth and the obtained GM and WM PV maps. The proposed method outperformed traditionally used methods by 33% and 34% in GM and WM, respectively.

Keywords: Bi-exponential model, MR Signal, partial volume correction.

1 Introduction

Magnetic resonance (MR) imaging is a non-invasive imaging modality allowing to detect changes in anatomy and is helpful in diagnosis of several diseases. It is particularly used in brain anatomy as it provides a high-resolution image of the intra cranial structures. Nevertheless, several artifacts arise during the acquisition such as partial volume effects (PVE), bias field and noise that may hamper tissue quantification. PVE may become critical when dealing with small structures like brain cortex where subtle differences in cortical thickness or volume can occur in presence of neurodegenerative

diseases such as Alzheimer's disease [1] or focal cortical dysplasia [2], and may yield to significant errors if not taken into account [3,4,5].

Standard approaches use tissues means and variances within maximum a posteriori classification framework to fit multiple gaussians modeling pure or even mixture of tissues onto the histogram [5,6,7,8,9]. The percentage of each tissue present in each voxel is thus a fractional content of each tissue type modeled by the statistical distributions of pure tissue and mixture voxels in the image.

Other approaches made use of two acquisitions and model the signal intensity of a voxel by two linear combinations of three mean pure tissue values, gray matter (GM), white matter (WM) and cerebrospinal fluid (CSF) [10,11]. However, the mean values estimated in the two images were not computed locally which make the method sensitive to radiofrequency (RF) inhomogeneities. As the authors stated in the paper, "the assumption that a pure tissue will give a constant signal response is a simplification in practice, particularly as field strengths effects can produce position dependent sensitivty" [10].

Here, we describe a model which stands on the physical properties of the signal of the acquisition, namely T1 and T2 relaxation time constants and proton density (PD) of the tissues and the parameters of acquisition TE (Echo Time) and TR (Repetition Time) (and TI -Inversion Time- for inversion recovery -IR- sequences). By using two co-registered images that nowadays may be obtained in a single acquisition such as in the new Fluid Attenuated and White matter Suppression (FLAWS) sequence [12], based on the MP2RAGE[13] technique, a bi-exponential model for MR signal is introduced. This model allows to retrieve the amount of GM, WM and CSF in each voxel of a presegmented intra cranial volume (ICV). We show how this problem leads to a linear system of two equations with two unknowns.

A direct and independent computation of GM/WM and GM/CSF fractional content maps is performed without assumptions about statistical properties of tissue values. This computationally inexpensive method is also robust to RF inhomogeneities as the signal intensities of a voxel in both images are identically biased.

2 Methods

2.1 Bi-Exponential Model for MR Signal

We modeled the MR signal with a linear combination of mono-exponentials with weighting as unknowns and representing the magnetizations of the two tissues considered in a voxel. Let's first consider the Spin Echo (SE) signal function for a single tissue as

$$s(\boldsymbol{x}, \boldsymbol{\Phi_{SE}}, \boldsymbol{T}) = M_0 e^{-\frac{TE}{T2}}(1 - e^{-\frac{TR}{T1}}) \tag{1}$$

where $\boldsymbol{x} = \{x, y, z\}$, $\boldsymbol{\Phi_{SE}} = \{TE, TR\}$, $\boldsymbol{T} = \{M0, T1, T2\}$ describe respectively the voxel position, the sequence parameters and tissue properties. M_0 is the longitudinal magnetization in the state of equilibrium and $T1$, $T2$ are respectively the longitudinal and transversal magnetization time constants. If we now consider two magnetic contributions from two different tissues α and β in a single voxel $\boldsymbol{x}$, the acquired signal is

written as

$$s(\boldsymbol{x}, \boldsymbol{\Phi_{SE}}, \boldsymbol{T_\alpha}, \boldsymbol{T_\beta}) = M_{0\alpha} e^{-\frac{TE}{T2_\alpha}} (1 - e^{-\frac{TR}{T1_\alpha}}) + M_{0\beta} e^{-\frac{TE}{T2_\beta}} (1 - e^{-\frac{TR}{T1_\beta}}) \quad (2)$$

Here, for a given voxel, $M_{0\alpha}$ and $M_{0\beta}$ are two unkwnowns and $T1$ and $T2$ are either known [14] or experimentally estimated. Thus, two acquisitions with different TE and TR result in a voxel-wise two equation system:

$$(S_{SE}) \Longleftrightarrow \begin{cases} s_1(\boldsymbol{x}) = s(\boldsymbol{x}, \boldsymbol{\Phi_{SE_1}}, \boldsymbol{T_\alpha}, \boldsymbol{T_\beta}) = \ k_{1\alpha} M_{0\alpha}(\boldsymbol{x}) + k_{1\beta} M_{0\beta}(\boldsymbol{x}) \\ s_2(\boldsymbol{x}) = s(\boldsymbol{x}, \boldsymbol{\Phi_{SE_2}}, \boldsymbol{T_\alpha}, \boldsymbol{T_\beta}) = \ k_{2\alpha} M_{0\alpha}(\boldsymbol{x}) + k_{2\beta} M_{0\beta}(\boldsymbol{x}) \end{cases}$$

with $k_{i,j} = e^{-\frac{TE_i}{T2_j}} (1 - e^{-\frac{TR_i}{T1_j}})$ where $i = \{1, 2\}$ denotes the acquisition number and $j = \{\alpha, \beta\}$ stands for the tissue. $k_{1\alpha}$, $k_{1\beta}$, $k_{2\alpha}$ and $k_{2\beta}$ are constant values across the image. The solution is:

$$(S_{SE}) \Longleftrightarrow \begin{cases} M_{0\alpha}(\boldsymbol{x}) = \ \dfrac{k_{2\beta} s_1(\boldsymbol{x}) - k_{1\beta} s_2(\boldsymbol{x})}{k_{2\beta} k_{1\alpha} - k_{2\alpha} k_{1\beta}} \\ \\ M_{0\beta}(\boldsymbol{x}) = \ \dfrac{k_{1\alpha} s_2(\boldsymbol{x}) - k_{2\alpha} s_1(\boldsymbol{x})}{k_{2\beta} k_{1\alpha} - k_{2\alpha} k_{1\beta}} \end{cases}$$

This can also be done with an IR sequence of parameters $\boldsymbol{\Phi_{IR}} = \{TR, TE, TI\}$. In this case, although the signal s is slightly different as shown in eq. (3), the bi-exponential model can still be solved as the SE system. Only $k_{1\alpha}$, $k_{1\beta}$, $k_{2\alpha}$ and $k_{2\beta}$ are different.

$$s(\boldsymbol{x}, \boldsymbol{\Phi_{IR}}, \boldsymbol{T}) = M_0 e^{-\frac{TE}{T2}} \left(1 - e^{-\frac{TI}{T1}} (2 - 2e^{-\frac{(TR - \frac{TE}{2})}{T1}} + e^{-\frac{TR}{T1}})\right) \quad (3)$$

2.2 Estimation of the tissue parameters

Although brain tissue parameters are currently well known [14] a large inter-indvidual variability may exist and they may need to be consequently estimated. This subsection explains how these information can be retrieved from a pair of acquisitions.

Proton Density To measure the proton density (PD) of a tissue relatively to another tissue, one can acquire a sequence with an infinite TR, or at least 5 times the $T1$ of the considered tissues. Then the ratio $\frac{S_{GM}}{S_{WM}}$ (where S_{GM} is the signal of a pure GM tissue) should give the same result as $\frac{PD_{GM}}{PD_{WM}}$.

T1 T1 measurement of a tissue α was made by finding the solution of $g(T1) = \frac{k_{1\alpha}}{k_{2\alpha}} - \frac{\mu_{1\alpha}}{\mu_{2\alpha}} = 0$ where $\mu_{i\alpha} = \frac{1}{|\Omega_\alpha|} \sum_{\Omega_\alpha} S_i, i = \{1, 2\}$ is the mean of tissue α in the i^{th} contrast image and Ω_α stands for the domain of pure tissue α.

2.3 Fractional content calculation

Signal magnitude M_0 must be positive and hence negative values are first set to zero. The preserved M_0 values are subsequently divided by the PD to compensate the lower water concentration in these tissues, the fractional content is eventually computed as :

$$f_{\alpha/\beta}(\boldsymbol{x}) = \frac{M_{0\alpha}(\boldsymbol{x})}{M_{0\alpha}(\boldsymbol{x})+M_{0\beta}(\boldsymbol{x})} = \frac{k_{2\beta}s_1(\boldsymbol{x})-k_{1\beta}s_2(\boldsymbol{x})}{s_1(\boldsymbol{x})(k_{2\beta}-k_{2\alpha})-s_2(\boldsymbol{x})(k_{1\beta}-k_{1\alpha})}$$

$f_{\alpha/\beta}(\boldsymbol{x})$ thereby represents the percentage of tissue α within the voxel $\boldsymbol{x}$ and it ranges between zero and one. This value is only valid $\forall \boldsymbol{x} \in \Omega_\alpha \cup \Omega_\beta$.

The method computes the fractional content at both boundaries of the GM, namely GM/WM and GM/CSF. To combine the two models, $f_{GM/WM}$ values are computed at the intersection of dilated GM and WM ground truth binary masks (radius 1). The aim of the study is to show the accuracy of the bi-exponential model, thus no segmentation step was included in our work. Likewise on the GM/CSF boundary yielding the $f_{GM/CSF}$ values. Otherwise, the fractional content in the remaining GM is computed as $max(f_{GM/CSF}, f_{GM/WM})$.

3 Experiments

3.1 Physical Phantom

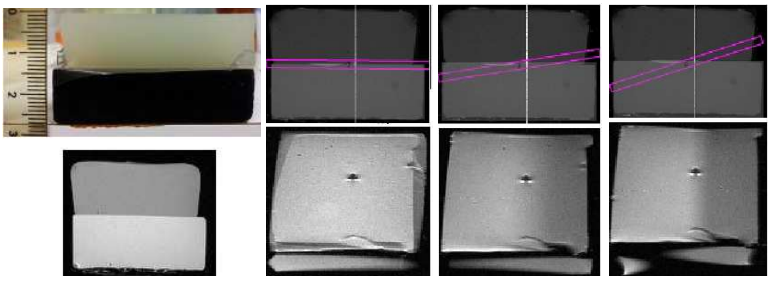

(a) DoubleLayer phantom (b) $\theta_0 = 0°$ (c) $\theta_2 = 10°$ (d) $\theta_4 = 20°$

Fig. 1. DoubleLayer physical phantom. (a) Picture (*top*) and SE imaging (*bottom*) of the phantom. India ink was added to the GM solution to visually differentiate the two gels. (b,c,d) Acquisition protocol to control partial volume effects. *Top* the tilt, *bottom* the resulting images for different inclination angles (SE, $TR/TE = 800/10ms$, slice thickness $e = 4mm$, FOV = $8cm * 6cm$, matrix = $128px \times 128px$).

The method was tested on a physical phantom composed of two gel-layers simulating respectively GM and WM tissue relaxation properties. The gels were made by a combination of gadolinium chelate and distilled water (eq. (4)). R_1 and C_{gado} are respectively the relaxivity and the concentration of the contrast agent.

$$T1 = \frac{1}{\frac{1}{T1_{water}} + R_1 C_{gado}} \tag{4}$$

Then, agar (2.5%) was added to the solution and warmed up. While cooling down, the solution jellifies. T2 was fixed as the concentration of agar was the same for the two gels. Thus, a DoubleLayer phantom simulating a flat GM/WM interface was obtained by varying the concentration of gadolinium chelate in the two solutions. The T1 obtained at 4.7 Tesla (T) were 903ms for WM and 1130ms for GM (see Fig. 1(a) *bottom*). These values are close to the values of brain WM and GM at 3T. Two microtubes as shown in the bottom of Fig. 1(b,c,d) are always present next to the DoubleLayer as a T1 reference.

SE images with different acquisition parameters were obtained on a Bruker Biospec 4.7T scanner (Bruker Biospin, Rheinstetten, Germany). In order to vary the partial volumed zone (PVZ), a first 4mm thick slice was acquired in the middle of the GM/WM interface (Fig. 1(b)). Then, the acquisition was incrementally rotated by a 5° angle, progressively reducing the PVZ with θ, the inclination angle. Each position was acquired twice, the first image with parameters $TR_1/TE_1 = 800/10ms$ and the second image with $TR_2/TE_2 = 3600/10ms$. These parameters were optimized by running Monte Carlo simulations and minimising the error on fractional contents for two tissues.

The actual size d of the PVZ has a theoretical value of $d = \frac{e}{tan(\theta)}$ where e denotes the slice thickness. Then, the PVZ was measured using the resulting GM fractional content map where the values range from zero in the WM to one in the GM as we move from left to right within the image. By denoting n the number of pixels in the slope (*i.e.* $f_{GM/WM} \in]0, 1[$) and r_x (0.625mm) the resolution in the x direction, $d_{exp} = nr_x$ gives an experimental value of d. In that way, the fractional content error was estimated.

3.2 Simulated MR data

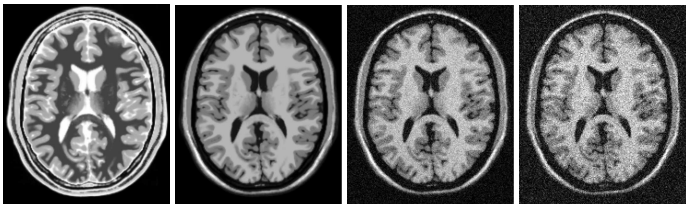

(a) (b) (c) (d)

Fig. 2. BrainWeb simulated images. (a,b) No noise and no RF inhomogeneties: example of the two contrasts obtained by simulating the two acquisitions in a typical FLAWS sequence. Next figures show contrast number 2 with 5% of noise, 20% of bias field (c) and 9% of noise, 40% of bias field (d).

We computed the GM and WM fractional content maps for different pairs of noise and field inhomogeneities. Then the Root Mean Squared Error (RMSE) was calculated between our maps and the BrainWeb Fuzzy maps for all the experiments. We used the BrainWeb Simulator [16] to build a database of FLAWS-like pairs of IR sequences such as those appearing in Fig. 2 (a,b). Each couple of simulated images was made using the following set of parameters: $TI_1/TR_1/TE_1 = 250/4000/2.3ms$, $TI_2/TR_2/TE_2 =$

$900/1900/1.6ms$ and flip angle $\alpha = 90°$ for both images. The choice of the parameters was based on the ones provided by the the original FLAWS paper [12]. The method was tested using 0, 3, 5, 7 and 9% as noise values and 0, 20 and 40 % as bias field values. The simulated data were not consistant with T1 and PD parameters indicated on the website [15] so we recomputed them all as section 2.2 describes. We found that the estimated parameters were sligthly different from the ones provided by BrainWeb. While a $\frac{PD_{GM}}{PD_{WM}}$ ratio of 1.04 is given, we estimated it at 1.12. $\frac{PD_{GM}}{PD_{CSF}}$ and $\frac{PD_{WM}}{PD_{CSF}}$ were also different. The T1 we obtained were $T1_{GM}/T1_{WM}/T1_{CSF} = 980/556/2947ms$ instead of $833/500/2569ms$.

4 Results

4.1 Physical phantom

An example of a bi-exponential response for a voxel shared between GM and WM is shown on Fig. 3, this response is clearly different from a pure GM or WM voxel. Fractional content maps are shown in Fig. 4(a,b,c,d) and must be put in relation with Fig. 1. As it was expected, the greater θ, the smaller the PVZ. Table shown in Fig. 4(e) summarizes these results and shows very good agreement between our measurements and the results from our model. Profiles for the different angles are plotted on Fig. 4(f). The lines intersect in the location $x = x_0 = 70$ and the fractional content is equal to 0.47, this value is defined by the acquisistion parameters of the first slice ($\theta_0 = 0°$).

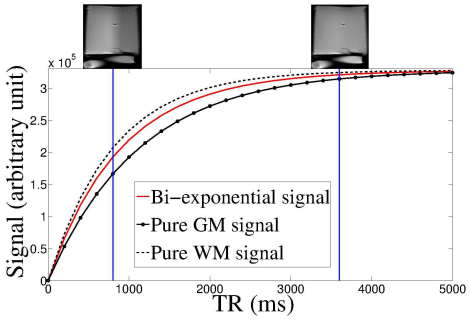

Fig. 3. Graphs of the bi-exponential signal compared to pure GM and WM tissues in a voxel where $f_{GM/WM} = 0.35$. The vertical lines refer to TR_1 and TR_2.

4.2 BrainWeb MRI Data

GM fractional content maps are shown in Fig. 5, the images show a strong robustness to RF inhomogeneities. As depicted on Fig. 6, our method shows a better RMSE between fractional content maps and BrainWeb references compared to the results reported by Shattuck [5], for instance Maximum A Posteriori (MAP) and Maximum Likelihood (ML). These results indicate that our method is more robust to field inhomogeneities than standard methods. The increase of the RMSE is only due to the increased noise.

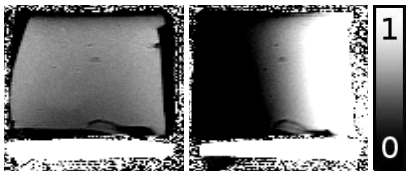

(a) 0° (b) 10°

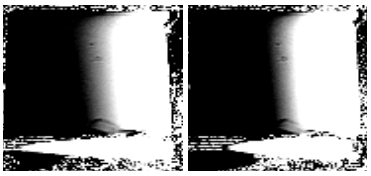

(c) 15° (d) 20°

$\theta(^\circ)$	5	10	15	20	25
d (mm)	45.72	22.69	14.92	10.99	8.58
d_{exp} (mm)	44.38	23.75	15.00	11.25	8.13
$d - d_{exp}$ (mm)	1.35	1.06	0.07	0.26	0.45
$d - d_{exp}$ (px)	>2	>1	<1	<1	<1

(e)

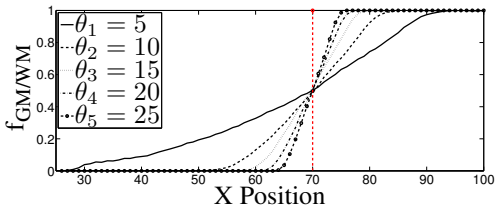

(f)

Fig. 4. (a,b,c,d) GM fractional content maps on the phantom for four angles. (e) Theoretical and experimental sizes of the PVZ for five angles. (f) Profile of the GM fractional content maps along a few WM-GM lines on the phantom. As expected, all the curves intersect at the same location: the center of rotation of the successive slices.

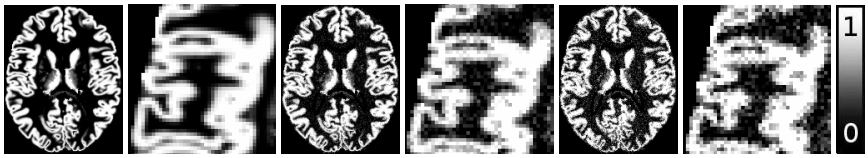

(a) (b) (c) (d) (e) (f)

Fig. 5. GM fractional content maps on the BrainWeb phantom. Experiments with 0% noise and 0% RF (a,b), 5% noise and 20% RF (c,d), 9% noise and 40% RF (e,f).

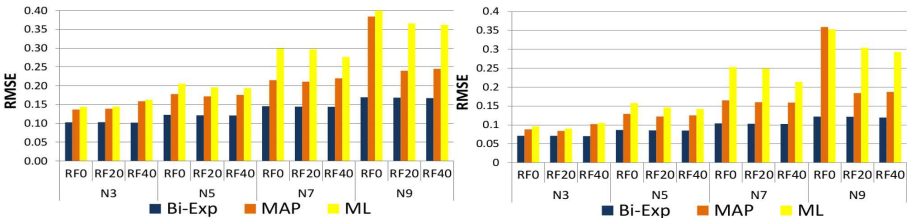

(a) GM (b) WM

Fig. 6. RMSE obtained on the BrainWeb database for GM and WM, Shattuck results are included for comparison. N and RF stand for the percentage of noise and field inhomogeneities. Our method is robust to RF inhomogeneities as we can observe plateaux when RF increases.

5 Conclusion

We proposed a fast method to accurately estimate fractional content of tissues using a bi-exponential model. It is intrinsically robust to RF inhomogeneities and outperforms

already existing and time-consuming approaches. Future work includes evaluation with thicker slices in a physical phantom and on actual T1-weighted and T2-weighted images as provided by a standard clinical protocol.

Acknowledgement. This work is partially funded by the "Région Bretagne".

References

1. Acosta, O., Bourgeat, P., Zuluaga, M.A., Fripp, J., Salvado, O., Ourselin, S.: Automated voxel-based 3D cortical thickness measurement in a combined Lagrangian-Eulerian PDE approach using partial volume maps. Medical image analysis **13**(5) (2009) 730–743
2. Chi-Ann Yang, Mostafa Kaveh, B.J.E.: Automated Detection Of Focal Cortical Dysplasia Lesions on T1-Weighted MRI using Volume-Based Distributional Features. In: Biomedical Imaging: From Nano to Macro, 2011 IEEE International Symposium on. (2011) 865–870
3. Ballester, Angel, M., Zisserman, A.P., Brady, M.: Estimation of the partial volume effect in MRI. Medical Image Analysis **6** (2002) 389–405
4. Leemput, K.V., Maes, F., Vandermeulen, D., Suetens, P.: Automated Model-Based Tissue Classification of MR Images of the Brain. IEEE Transactions on Medical Imaging **18**(10) (1999) 897–908
5. Shattuck, D.W., Sandor-leahy, S.R., Schaper, K.A., Rottenberg, D.A., Leahy, R.M.: Magnetic Resonance Image Tissue Classification Using a Partial Volume Model. NeuroImage **13** (2001) 856–876
6. Cuadra, M.B., Cammoun, L., Butz, T., Cuisenaire, O., Thiran, J.p., Member, S.: Comparison and Validation of Tissue Modelization and Statistical Classification Methods in T1-Weighted MR Brain Images. IEEE Transactions on Medical Imaging **24**(12) (2005) 1548–1565
7. Santago, P., Gage, D.: Statistical models of partial volume effect. IEEE Transactions on Image Processing **4** (1995) 1531–1540
8. Tohka, J., Zijdenbos, A., Evans, A.: Fast and robust parameter estimation for statistical partial volume models in brain MRI. NeuroImage **23** (2004) 84–97
9. Bricq, S., Collet, C., Armspach, J.: Unifying framework for multimodal brain MRI segmentation based on Hidden Markov Chains. Medical Image Analysis **12** (2008) 639–652
10. Thacker, N., Jackson, A., Zhu, X., Li, K.: Accuracy of tissue volume estimation in NMR images. Proceedings of MIUA, Leeds, UK (1998)
11. Rusinek, H., de Leon, M.J., George, A.E., A., S.L., Chandra, R., Smith, G., Rand, T., Mourino, M., Kowalski, H.: Alzheimer disease: Measuring loss of cerebral Gray Matter with MR imaging. Neuroradiology **178** (1991) 109–114
12. Tanner, M., Gambarota, G., Kober, T., Krueger, G., Erritzoe, D., Marques, J.P., Newbould, R.: Fluid and white matter suppression with the MP2RAGE sequence. Journal of Magnetic Resonance Imaging **35** (2011) 1063–1070
13. Marques, J.P., Kober, T., Krueger, G., van der Zwaag, W., de Moortele, P.F.V., Gruetter, R.: MP2RAGE, a self bias-field corrected sequence for improved segmentation and T1-mapping at high field. NeuroImage **49**(2) (2010) 1271 – 1281
14. Rooney, W.D., Johnson, G., Li, X., Cohen, E.R., Kim, S.g., Ugurbil, K., Springer, C.S.: Magnetic Field and Tissue Dependencies of Human Brain Longitudinal 1H2O Relaxation in Vivo. Magnetic Resonance in Medicine **57** (2007) 308–318
15. `http://www.bic.mni.mcgill.ca/brainweb/`
16. Cocosco, C., Kollokian, V., Kwan, R.S., Evans, A.: BrainWeb : Online Interface to a 3D MRI Simulated Brain Database. NeuroImage, Proceedings of 3-rd International Conference on Functional Mapping of the Human Brain, Copenhagen, May 1997 **5**(4) (1996) S425